Helvetica Physica Acta, Vol. 60 (1987) 577–593 0018–0238/87/040577–17$1.50 + 0.20/0

A low frequency field cycling experiment for relaxation dispersion measurements

By B. Borcard

University of Geneva Laboratoire de Resonance Magnetique 1254-JUSSY (Switzerland)

(6. VI. 1986)

Abstract. A field cycling technique, suitable for the measurement of T_1 against Larmor frequency, down to frequencies as low as 1 Hz, is described. The sample's magnetization is cycled from a polarization field to a relaxation field, variable from 80 mT to 23 pT. The free induction decay is observed in the earth's magnetic field. The cycle is repeated automatically to follow the evolution of the magnetization in the relaxation field for selected values of this field. T_2 in the earth field is an additional information. The sample's size is 18 cm^3 for a 300 signal to noise ratio on water. The accuracy on T_1 measurements can reach 1% as shown on some dispersions of the relaxation of water due to the scalar relaxation process between ^1H and the few naturally occurring ^{17}O nuclei (natural abundance: $3.7 \cdot 10^{-4}$).

Nuclear magnetic relaxation dispersion becomes an important tool for the knowledge of dynamic properties of heterogeneous systems (exchange and correlation times determination) [1]. Different approaches have been proposed [2, 3, 5, 6, 7]; the one proposed here makes use of the long experience of the laboratory on NMR in the earth's magnetic field [4]. The relaxation times T_1 are measured in Larmor frequencies from 1 Hz to 3 MHz, which represents at least two orders of magnitude lower than previously described equipments [5, 16, 31]. The whole procedure is automated from the insertion of the sample to the final relaxation dispersion curve.

The "field cycling" method

One of the neatest ways of solving the problem of the measurement of the dependence of the relaxation times on Larmor frequency is unquestionably the 'field-cycling' method which can take many different forms. Their common feature is the use of separate relaxation and observation fields, this last being taken at a fixed value. A cycle will be described between both fields: relaxation from some initial state in the first field, evaluation of the residual magnetization at a given time in the second one and back to the first. The cycle will be repeated until the equilibrium magnetization in the relaxation field is reached.

Different means of describing the cycle have already been used. If the spins stay in the observation field for a time much shorter than T_1 in the lowest of the two fields, it will be possible to measure T_1, or even T_2, in a single sequence of duration $\sim T_1$ [5]. Otherwise, the full cycle will be described many times [6, 7], and, if n points are measured on a magnetization curve, the total time for an experiment will be 3 to $5nT_1$ depending on the waiting time between two cycles.

To switch from one field to the other, numerous solutions can be considered. The two fields' areas may be physically separated by some distance, the sample being transferred from one to the other, for instance, by pneumatic propulsion [8] or fluid flow if the sample is liquid [9]. In these techniques, large mechanical stresses are applied to the sample and their applications stay limited. Both fields can be generated by the same coil, different currents yielding the two field values. This coil must meet drastic conditions: short time constant to allow fast field switchings and homogeneous field distribution (currently 10^{-5}) in order to observe the FID and echoes in the observation phase. It can be a superconducting [15] or a copper [6] coil. Using two different coils can also be considered, their main fields will be in the same area, but one will provide a homogenous field for observation and the other, a short time constant. The directions of these fields can be different; opposite directions have already been used [5]. This two-coil arrangement gives the best flexibility. The experiment described here is derived from this last solution, the relaxation field is produced by a coil whose homogeneity does not need to be very high, it only settles the field accuracy and, considering that the accuracy on T_1 is rarely better than 1%, this accuracy was also chosen for the Larmor frequency. The second field is merely the earth's field and thus does not need any magnet at all.

The cycle

The cycle follows a classical scheme [31, 10], with 3 phases: polarization of magnetic moments, relaxation and observation of the residual magnetization. Figure 1 shows the fields' states and the evolution of the magnetization in these various phases.

Polarization phase

The polarizing field (B_p) is applied to the sample's magnetic moments for a time such that we can consider the sample magnetization to be close enough to equilibrium. This condition must be fulfilled only for a maximum sensitivity, but, at the expense of reduced sensitivity, any polarization time can be used. The macroscopic magnetization is then M_{zp} in the B_p direction.

Relaxation phase

The field B_p is removed and replaced by the relaxation field B_r in the same direction. If it is held during the time t, the resulting magnetization will be:

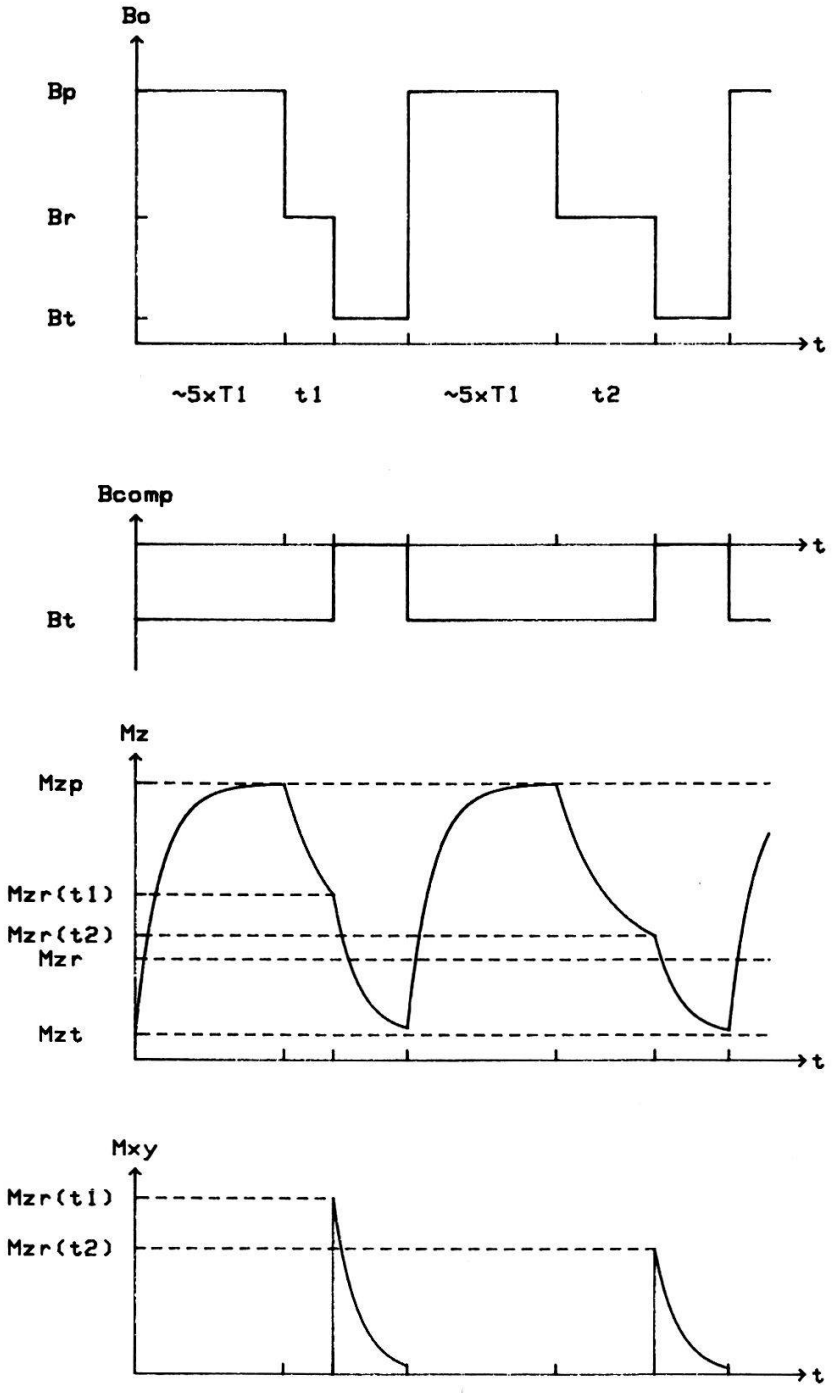

Figure 1
The field sequence begins with the polarization field (B_p) applied for a $5T_1$ duration (magnetization M_{zp}), the value is changed to the relaxation field (B_r), in which T_1 is to be measured, for a time t_1, the magnetization becomes $M_{zr}(t_1)$. B_r is switched off, remains B_t, the earth field whose direction is perpendicular to B_p and B_r. The magnetization precesses around it, the initial amplitude of the FID measures the residual magnetization $M_{zr}(t)$. The earth field is compensated during the first two phases (B_p, B_r) to provide relaxation field values lowest than 50 μT. The cycle is repeated for a stay time t_2 in the field B_r.

$M_{zr}(t) = (M_{zp} - M_{zr})e^{-t/T1} + M_{zr}$ (where M_{zr} stands for the equilibrium value of magnetization in B_r field = $M_{zr}(\infty)$.

Observation phase

The field B_r is switched off. If the experimental arrangement has been made in such a way that the earth field is perpendicular to B_r and B_p, the residual magnetization $M_{zr}(t)$ is going to precess around the earth's field B_t with the Larmor frequency: $\nu_t = \gamma B_t$ (1982 Hz at our location). This magnetization, which is now transverse, M_{xy}, disappears with the time constant T_2 relevant to the earth's field.

This precession movement of the magnetization induces a current in a detection coil whose axis is perpendicular to both B_r and B_t. This current, amplified and filtered, provides the measure of the residual magnetization $M_{zr}(t)$.

Earth field compensation

Properly speaking, this does not constitute a phase of the cycle, but, as the aim is to reach the lowest relaxation fields, any outside contribution must be cancelled. Thus, the earth's field is compensated for during the first two phases.

Technical description

Coils set (Fig. 2a and b)

Each of the three space axis are occupied by a group of coils whose specifications are the following.

– Field coils: a single short solenoid coil (Outside diameter: 17.7 cm, inside diameter: 6.9 cm length: 10.1 cm) produces both B_p and B_r fields. Its electrical features are $L = 0.5$ H, $R = 15\ \Omega$, field-current coefficient: 240 G/A. It has been calculated for a maximum deviation of 1% of the field value along the cylindrical sample. Its cooling is by forced air through a channel enclosing the coil.

– The receiving coil is a simple solenoid, internal diameter: 2.8 cm, external diameter: 4.5 cm, length: 5 cm, with 4800 turns of enamelled copper wire (0.2 mm diameter). Its induction coefficient is 0.9 H for a Q factor of 35 at 2 kHz and a field-current coefficient 1100G/A. The sample that just fits inside has a 18 cm^3 usable volume. Lower volumes can be used with dedicated coils (smaller inside diameter, thinner wire, . . .) with increased field-current coefficient (the signal amplitude is proportional to this coefficient [11]). The coil Q factor is of less importance as it can be generated in the preamplifier circuit at any chosen value up to at least 1000.

– The earth's field is compensated for by Helmoltz coils, 28 cm in diameter, with 196 turns each. The field in the homogenous region is 18 G for 1 A. An adjustable resistor bridge symmetrizes the currents in each coil for a better

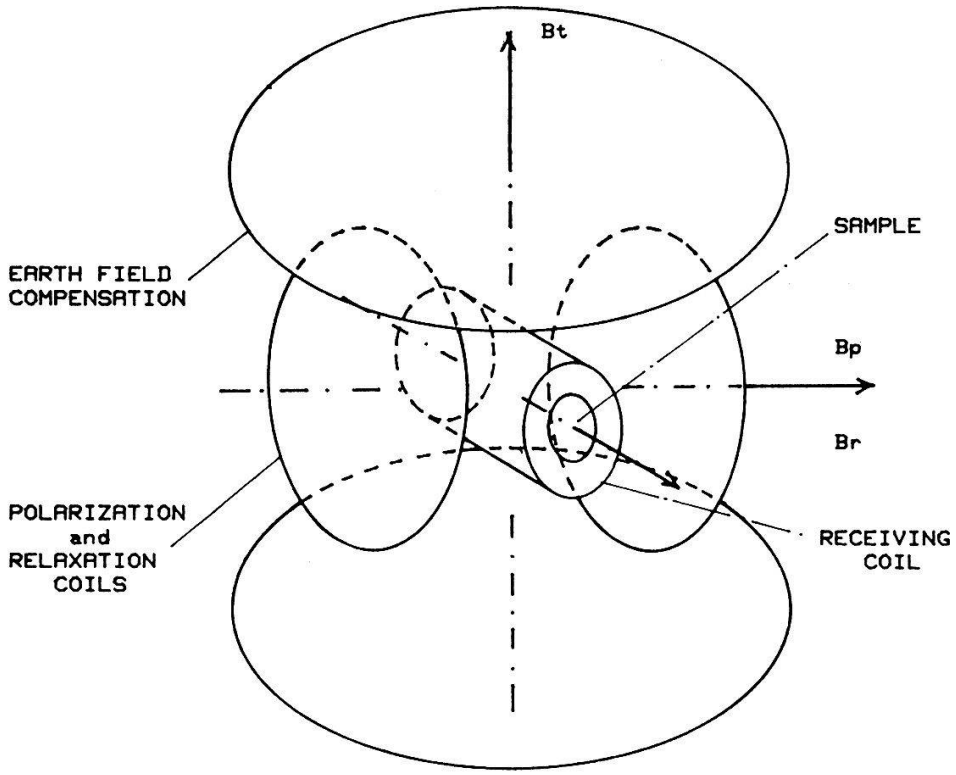

Figure 2
The coil arrangement. A solenoid which contains the sample is the receiving coil. Polarization and relaxation fields are provided by the same coil. Two flat coils compensate the earth field and are aligned with it.

homogeneity. The residual gradient has been measured to be 20 μG on the whole sample for a field value of 0.46 G.

– Probe shielding against AC magnetic fields is essential. Owing to the quite large size of the detection coil, such fields can induce interference voltages even in an area chosen to be far from any large town (15 km) and from any human activity (500 m). They are generated by eddy currents flowing in the ground and whose spectrum contains the Larmor frequency.

Shielding techniques against low frequency magnetic fields were recently developed with the applications of SQUID to the measurement of "evoked" fields in living bodies [12]. The shielding can be considered as a resistor-inductance circuit which forms a low-pass filter whose cut-off frequency depends essentially on the shielding size, the material conductivity and its thickness. A cubic box, 60 cm by side, made of 6 mm thick welded aluminium, with just a 10 cm diameter opening to insert the sample, has a cut-off frequency of 10 Hz and a 2 kHz attenuation of more than 50 dB. The minimum usable size for the shielding is determined by the interaction between box walls and the variable fields generated inside the measuring head: fields' switchings and fields induced by the sample in the receiving coil. This coupling between the coils and the shielding depends on the leakage fields of the coils. For solenoid type coils, a practical rule of thumb will at least be a factor 2 between the coil's and the shielding's corresponding sizes. An additional feature of this shielding is the protection against electrical fields ('Faraday cage').

– The earth's magnetic field is the detection field, a location where it is quite homogenous has been chosen. Much less ideal locations than this laboratory [4] are still practicable. The field gradient must be low enough for a FID to be observable (~8 mG/m for a 100 ms FID decay time). Such conditions can be found a few metres from a building, assuming that no iron pipes or pieces of ferromagnetic materials are buried in the soil. The T_2 information is then lost, but a Carr–Purcell pulse sequence makes it possible to recover it.

The associated electronics

Figure 3 describes the electronics which connected to the coils provides the experimental points for the dispersion curves.

The fields sources. Each field (B_p, B_r and $-B_t$) possesses its own generator. Field B_p is derived from a constant voltage source ($U_{max} = 60$ V), the current is 3.5 A for a polarizing field of 840 G.

The relaxation field comes from a programmable voltage and current generator (HP6034A). In the current regulation mode, the time for the power supply to reach a new current value is too long for the experiment and the voltage regulation mode is used. The voltage is determined by computer software. For field values lower than 10 G, the source is transformed into a current generator by adding a 1 kΩ, time and temperature stable resistor in series with the coil. This has the added advantage of deriving higher voltages from the power supply, which increases the accuracy. If the field is still lower, from 0.1 G, the resistor is changed to 100 kΩ.

A constant current generator feeds the earth field compensation coils. It must be very well designed for stability and accuracy, as the precision for the very low relaxation fields depends primarily on this compensation. A very stable reference voltage is the heart of this home-built generator [13].

Field switching. The growth of the field B_p is not critical, as we shall stay in this field for at least $3T_1$, the lengthening of this duration will compensate for the loss of magnetization. The field change-over from B_p to B_r must be very fast compared to the shortest T_1 (which is T_1 in the relaxation field, as $B_r \leq B_p$). It must be noticed that, if B_r of the same order of magnitude than B_p is investigated, the magnetization will evolve between M_{zp} and M_{zr} whose values are very similar, which is against a good accuracy on T_1 determination. The magnetization was selected to go from M_{zp} to $-M_{zr}$, if $|M_{zr}| \geq M_{zp}/20$. Thus, the total variation of magnetization during the relaxation phase does not change much with the field value, going from $2M_{zp}$ (for $M_{zr} = M_{zp}$) to $0.95\,M_{zp}$ (for $M_{zr} = M_{zp}/20$). The accuracy of the measurements is then quite insensitive to B_r. From a practical point of view, this choice implies additional constraints. The longitudinal field will cross through zero and if the earth's field is present in the transverse direction during the field reversal, the magnetization can change its orientation, resulting in a loss of signal. In order to avoid it, the earth's field is cancelled during the first two phases. Still, the zero field crossing must be very fast (non adiabatic

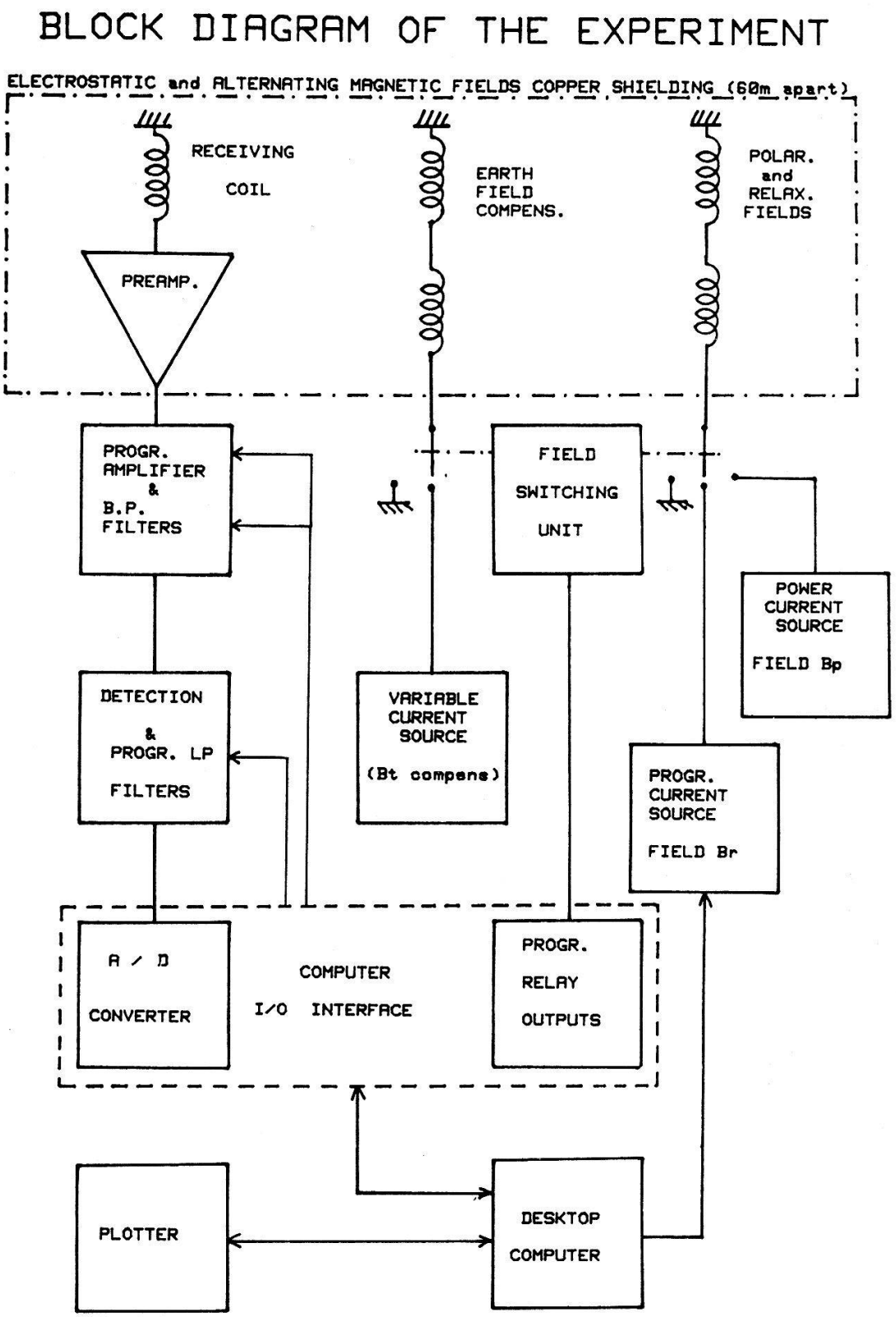

Figure 3
Block diagram of the experiment.

condition). A circuit that transfers energy from the coil to a capacitor helps this delicate crossing [14]. The field change-over rate is 80 T/s for a total field reversal time of 1 ms.

To switch off the field B_r in the presence of the earth field is the most critical operation. The non-adiabaticity criterion ($\gamma\, dB_r/dt \gg v_t^2$) must be carefully produced down to zero field (which means a field such that $\delta B_r/B_r$ (B_r relative inhomogeneity) $\times B_{rr}$ (residual field) is much lower than $1/\gamma T_2$ (the line width), for instance, T_2 of water is around 2s and $1/\gamma T_2 \sim 19\,\mu$G, the field coils relative inhomogeneity in this experiment is $\delta B_r/B_r = 10^{-2}$, the residual field must be much lower than 1.9 mG, which represents 4.2×10^{-6} of the maximum field). Two different approaches can be considered; energy transfer from the coil to a capacitor [14, 15] and energy dissipation in a resistor, which can be the coil resistance. Both schemes are shown on Fig. 4. The ideas are very simple, for circuit a), just after S_1 is open, S_2 is closed and L, C, R form a damped oscillating circuit. When the coil energy is completely transferred to the capacitor, S_2 is open. A serious improvement to this technique is to pre-charge C at a potential U_0 (sign opposite to U). In circuit b), the coil discharges its energy through $(R + R_1)$, but instead of going towards zero potential, it discharges down to V_z (sign opposite to U). V_z is generated by the current flowing in a Zener diode and S_2 is a simple diode.

Both techniques yield similar switching times for the same voltage to handle (see Appendix). The maximum voltage permissible across the switching device is the limiting factor; 1000 V is thought to be a maximum for semi-conductors or relays (vacuum relays can withstand higher voltages, but are not bounce-free and thus not applicable here). The energy dissipation technique has been the choice for this experiment. First, its ability to parallel circuits in order to decrease the switching time and the components strains allows very fast turn off rates with a very high reliability (so far, more than 10^6 fields switchings without a breakdown). Then, after S_2 opens, some energy is left in the coil, this residual energy is orders of magnitude higher in the capacitor circuit through the following process. Stray capacitances are also charged during the transfer process, but cannot be separated from the coil. Owing to the line length, this capacitance is quite high (~6 nF) and 80 mA are left in the coil. The Zener residual current is much lower, even if the

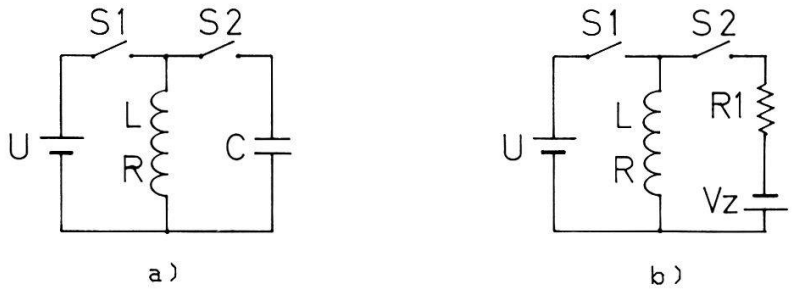

Figure 4
(a) Switching by energy transfer from the coil to a capacitor. S_1 is open and S_2 closes the LC circuit. S_2 is open when all the energy is transferred to the capacitor (a quarter of a period of the LC circuit). C is discharged by any external mean. (b) Energy dissipation. the energy is dissipated in resistor $R + R_1$, from the potential U to the potential $-V_z$.

Zener resistance increases as the current decreases, but the diode still conducts to around 10 μA. These leakage currents are suppressed by damping the LC circuit (L: coil, C: stray capacitance) with a resistor of slightly higher value (40%) than the critical one ($R_c = \frac{1}{2}(L/C)^{1/2}$), which insures the faster return to zero energy.

The final design is that of Fig. 5, three cells are paralleled, resulting in a switching time from maximum field to zero of less than 1 ms. Switch S_1 is a mercury wetted relay. Semi-conductor switches cannot be used here as they exhibit high leakage currents (milliamperes for Amperes switching transistors), which forbid access to low relaxation fields (1 kHz Larmor frequency for each mA leakage current). Compensation of this residual field [16] is troublesome, as the leakage current is highly temperature dependent.

Detection

The signal induced in the receiving coil at Larmor frequency must be amplified and filtered. The low-noise amplifier [17] with a high input impedance (coil impedance at resonance: $QL\omega = 200\,\text{k}\Omega$) is located near the coil set. This closeness avoids long lines (60 m) with inherent earthing problems. A special feature of this preamplifier is the presence of a controlled regeneration loop which acts as a Q multiplier (Fig. 6). The coil's Q factor is determined by the regeneration control (~100 for normal operations) and can be increased to more than 500 for slowly decaying FIDs ($T_2^* > 2$ s) to improve the signal to noise ratio.

The signal is carried from the coils location to the main building, where it is filtered and detected (4 kHz component removed). It should be mentioned that phase detection is not applicable here [18], because of the lack of a phase reference. The earth field exhibits small variations (some μG) on a time range of milliseconds, and using a frequency stable reference will introduce articial factors into the decay of the signal which will prevent accurate T_2 determination and curve adjustments. The signal to noise ratio for a 18 cm^3 water sample amounts to 300. All settings, gain, filters characteristics are manually or remotely accessible from the computer, which also generates the time sequence for a full dispersion curve. The data from the A/D converter are stored in the mass memory for further processing.

Data processing

A standard dispersion is composed of 24 field values spaced on a logarithmic scale (4 by decade), each with 30 FID for different residence times in the

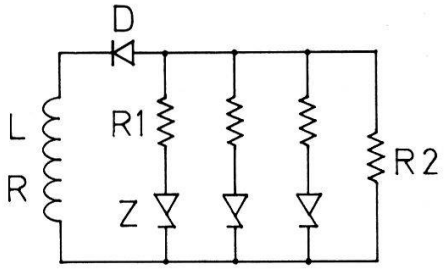

Figure 5
Practical circuit with 3 parallel cells. D: 1N4007, R_1: 120 Ω, R_2: 12 kΩ, Z: 7xBZX70C75 (Zener and transient suppressor, non repetitive peak power dissipation 700 W).

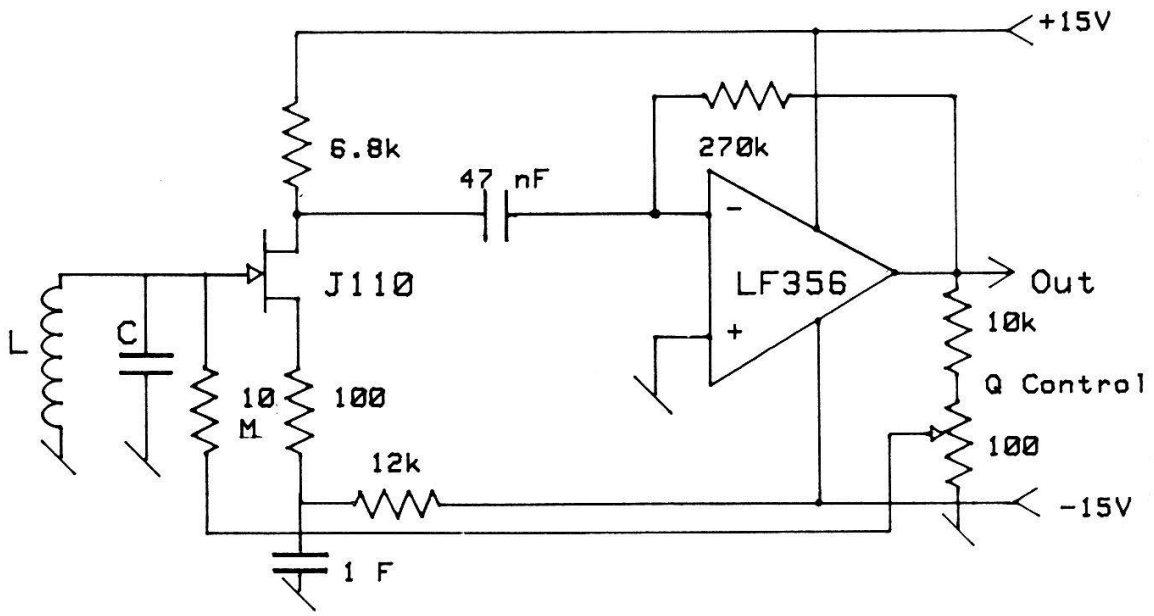

Figure 6
Low noise and high input impedance preamplifier, the regeneration loop controls the coil Q. Gain from 1500 to 30 000 (depending on the Q control), input noise voltage from 1.5 nV/√Hz at 200 kΩ input impedance to 4 nV/√Hz at 2 MΩ impedance (high Q).

relaxation field. For each field value, the 15 FID of largest amplitudes are added (50 points by FID) and T_2 is derived from this sum. For the adjustment of the exponential curve to the experimental points, the Simplex procedure of Nelder and Mead [19] is used. If n parameters are to be fitted, this method searches, in a $(n+1)$ dimension space, the minimum on the representative surface of the chosen convergence criterion (χ^2 has been chosen) by quasi geometric means. This procedure has proved very efficient and can be applied to any function. For multi-exponential signals, Simplex is generally better (lower χ^2) than all the other methods we have experimented (20, 21, 22), but it is time-consuming.

From this computed T_2 value, a new fit will give the initial amplitude for each FID. T_1 is still derived from this set of initial amplitudes by the Simplex procedure. The dispersion curve is drawn from T_1 values for all fields. Some theoretical function is fitted to the dispersion curve depending on the interaction involved. If we are concerned with protein solutions, empirical expressions used in dielectric relaxation, like the Cole-Cole one, can be fitted [7]:

$$\frac{1}{T_1} = \frac{1}{T_{1W}} + D + \frac{A[1 + (\omega\tau)^{\beta/2} \cos(\beta\pi/4)]}{1 + 2(\omega\tau)^{\beta/2} \cos(\beta\pi/4) + (\omega\tau)^{\beta}},$$

where T_{1W} is the relaxation time of the solvent, D a constant bound to an unobserved high field dispersion, A is the amplitude to the dispersion, ω the Larmor pulsation for the field in which T_1 is measured, τ is the correlation time for the process responsible of the dispersion and β an arbitrary constant, whose value lies between 0 and 2, which takes into account the width of the dispersion. Four parameters must be fitted (D, A, τ, β) and even seven in the case of two separate dispersions (D, A, τ, β, A', τ', β').

Applications

The applications are widely dependent on the field range and T_1 achievable values. The origin and position of these limitations must be set precisely.

Limits for the fields

At present, the power supply can deliver only 200 W, which imposes the high field limitation (3 MHz). Higher fields can be achieved at higher power levels, but dissipation increases with the square of the field and fields greater than 5 MHz, in Larmor frequency units, will need a more efficient coil cooling, using a higher-density fluid (water, liquid nitrogen, . . .).

On the low field side, the earth field compensation is the critical parameter. Any external field residue shows off from two different ways. First, the component along the relaxation field adds or subtracts to it, introducing an error in the relaxation field value. Secondly, if a part is perpendicular to the relaxation field and becomes of the same order of magnitude as the latter, the magnetization will precess and reorient along the field sum direction, resulting in a loss of magnetization and a two-exponential decay (resp. T_2 and T_1 in the sum field). This feature can be useful to align the compensation and earth fields accurately. The compensation field homogeneity is slightly degraded by desymmetrizing the currents into each coil, the T_2 part decay becomes T_2^*, shorter than T_2, which will be clearly different from the T_1 decay. Minimizing this short decay time component ensures an accurate alignment of the earth and compensation fields. A 0.03° lining up error results in a 1 Hz deviation of the relaxation Larmor frequency. It must be mentioned that the mean diurnal variation of the earth's field amplitude is of this order of magnitude, which means that, when the need to measure at very low fields (<10 Hz) arises, the compensation must be adjusted just before beginning the experiment.

Relaxation times limits

Severe limitations occur from the shortest observable FID. This minimum decay time is related to the response time of the receiver, which is imposed by the bandpass characteristics of the various filters, including the receiver coil. This bandwidth, however, determines the signal to noise ratio and a compromise must be found. Typically, the signal must decay in more than 40 ms to allow T_1 measurement. As T_2 at 2 kHz is generally shorter or equal to T_1, this minimum decay time supersedes the usual limitation arising from field switching rates [23]. Magnetic field homogeneities and radiation damping [24] shortens the decay for $T_2 > 2$ s; up to this value, accuracy on T_2 is ±5%, and drops rapidly at higher T_2. T_1 precision can be better, as shown later. These T_1 and T_2 ranges are particulary well suited to the analysis of liquids or samples with liquid-like relaxation (gels, tissues, . . .).

Correlation times from 10^{-2} s to 10^{-8} s and their related correlation functions

like those for the tumbling of large molecules in a solvent, can be determined by dispersion of the relaxation in this field range. An extensive study of the dynamics of fibrinogen (a large blood protein), both in solution and gelled by external agents has been performed [25]. In the same order of ideas, the evaluation of diffusive processes on large surfaces is within the scope of this experiment [26]. Modulation of scalar coupling between two different spins by the exchange of one of the coupled nuclei is a relaxation process, which can be described, neglecting local field and slow exchange effects, by [27]:

$$\frac{1}{T_{1IS}} = \frac{4}{3} S(S+1) p \frac{A^2 \tau_e}{1 + (\omega_I - \omega_S)^2 \tau_e^2},$$

where p is the $S(>\frac{1}{2})$ spin concentration, $A = 2\pi J_0$, J_0 the coupling constant between spin S and I, ω_S, ω_I the Larmor pulsations of spins S and I and τ_e the exchange time of spin I (or S). The dwell time τ_e of the nuclei of spin I on the molecule can be derived from a dispersion curve. As J_0 values are generally not very high (~100 Hz), the dispersion's height is significant only for slow exchanges ($\tau_e > 10^{-6}$ s) and is observable in the low Larmor frequency region ($[\nu_I - \nu_S] < 10^5$ Hz). A typical case of such a relaxation dispersion is that due to the $^1H - ^{17}O$ coupling in water [28, 29]. Here, $p = 3.7 \times 10^{-4}$, $S = \frac{5}{2}$, $I = \frac{1}{2}$, $J \sim 90$ Hz, $(\omega_I -$

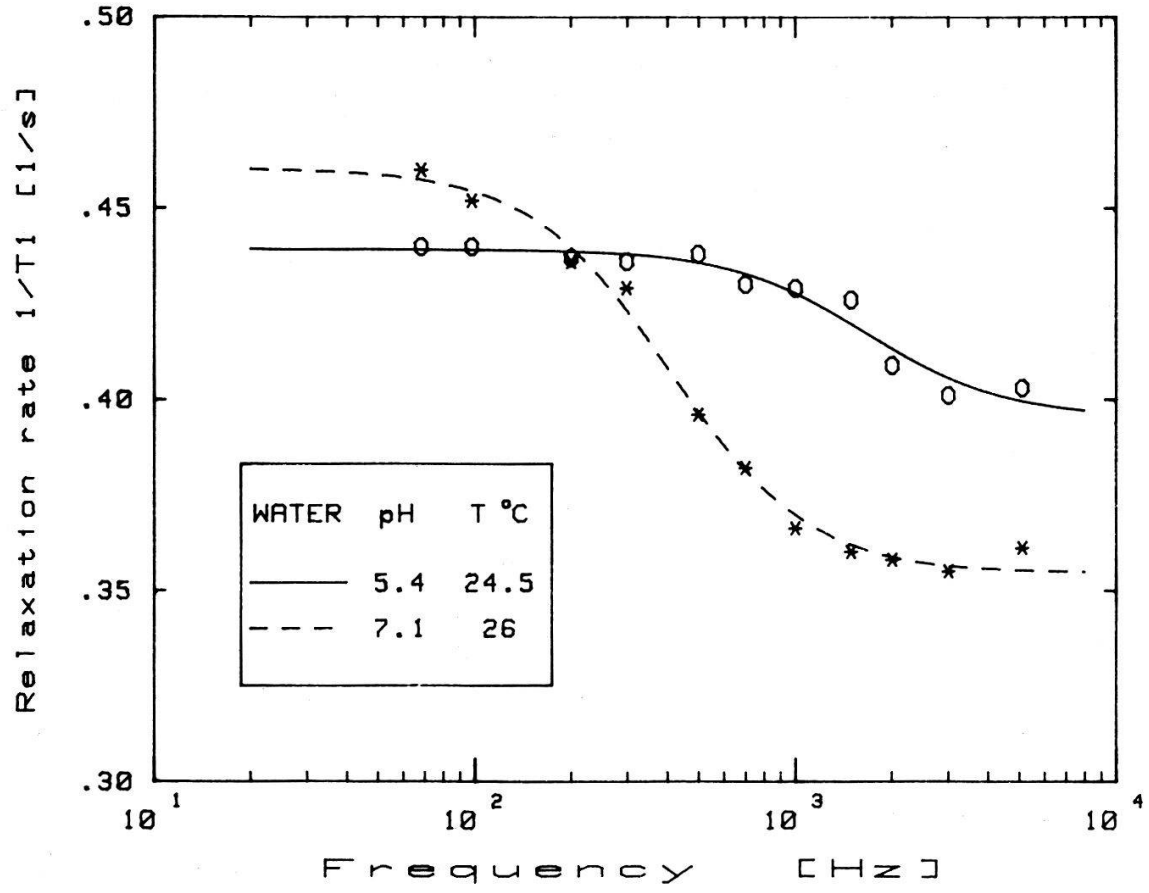

Figure 7
Relaxation dispersion curves of water, for two different pH values. The centre of the dispersion region is inversely proportional to the exchange time τ_e of protons on the water molecules and the dispersion height is proportional to τ_e.

$\omega_S) = 0.864\,\omega_I$. The residence time of a hydrogen atom on a water molecule widely depends on the pH value, Fig. 7 shows the dispersion of the relaxation for two pH values. The dwell time change appears as a displacement of the dispersion centre ($\propto 1/\tau_e$) as well as an alteration of its amplitude ($\propto \tau_e$). For weak or large pHs ($4.5 > \mathrm{pH} > 9.5$), the amplitude is so small that the dispersion becomes unobservable (fast exchange).

For pH 5.4, in the high field region, $T_1 = 2.48$ s and in the low field region, $T_1 = 2.27$ s, the total variation amounts to 8.5%, it can be seen that the dispersion is well resolved, which sets T_1 measurements accuracy to ±1%. A detailed analysis of the hydrogen atom exchange in natural water as seen by relaxation dispersion will soon be published [33]. Similar exchange time determinations have been carried out on the $^{14}N - {}^{1}H$ interaction into various molecules (urea, acrylamid, amino-acids) [32].

A general review on the field cycling techniques has recently been published [31]. The device described here is complementary to those therein. The general principles are shared, but the main feature of this one is to reach very low Larmor frequencies, and a great deal of work is to be done in this area. It may be noticed that relaxation by scalar coupling in the ammonium ion leads to a dispersion at a frequency lower that 1 Hz, owing to an exchange time of the order of 300 ms [32]. This dispersion is outside the present capabilities of this experiment and further improvements are to be considered.

Appendix

The time necessary to eliminate the energy from the coil is calculated from the equations for the circuits of Fig. 4(a) and (b). The choice of optimum parameters for both systems will help to select the best coil for fast switching.

Capacitor energy transfer

The equation for the current flowing in this circuit is classical:

$$Ri + L \cdot di/dt + 1/C \cdot \int i\,dt = 0,$$

whose solution is:

$$i = \exp(-Rt/2L) \cdot (C_1 \cos \omega t + C_2 \sin \omega t),$$

where: $\omega = (1/LC - R^2/4L^2)^{1/2}$, constants C_1 and C_2 are calculated from the initial conditions: $i = I_0$ (the current in the coil during steady state) and $U_c = U_0$, if the capacitor is initially charged to U_0 by some external voltage source. Solution writes:

$$i = \exp(-Rt/2L) \cdot \{I_0 \cos \omega t - [(U_0 + RI_0/2)/L\omega] \sin \omega t\}. \qquad (1)$$

The switching time τ is the time when $i = 0$:

$$\tau = 1/\omega \cdot \text{arctg}\,[L\omega I_0/(U_0 + RI_0/2)]. \tag{2}$$

The maximum voltage across the capacitor (and the switching device) is derived from energy considerations:

$$U_{max} = [(LI_0^2 + CU_0^2)/C]^{1/2}. \tag{3}$$

To determine the components' values, the first choice to be made is the maximum voltage that the switching device can withstand, this sets the maximum capacitor value from (3). Finally, the switching time is given by (2). The evolution of τ for the magnet coil in this experiment is shown on Fig. A.1. $U_{max} = 1000$ V, which is the maximum safe voltage for the relays, has been chosen and C is the optimum value at the highest switched current (5A). It appears that the higher U_0, the faster will be the switching time (U_0 drives a phase factor in (1)).

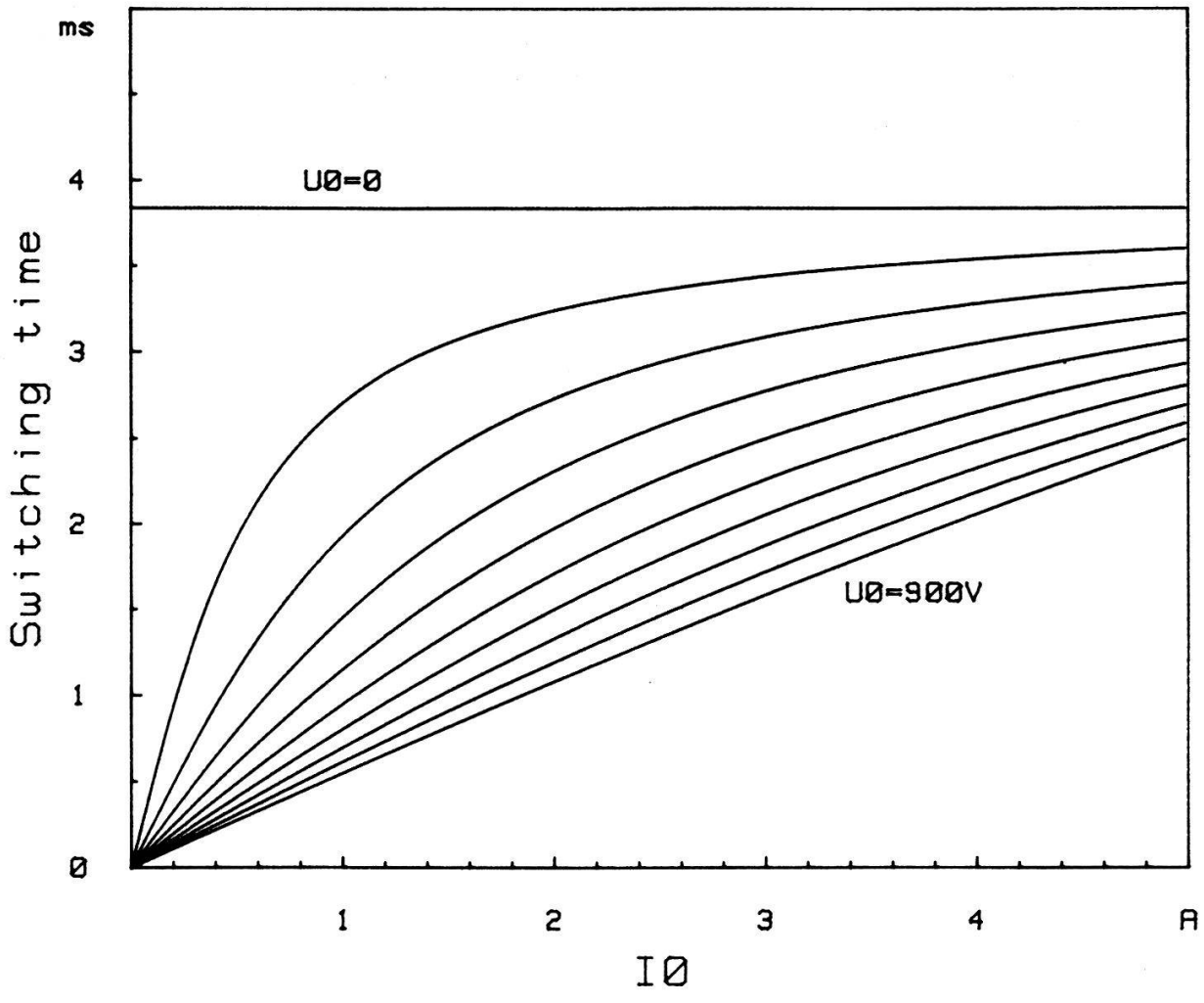

Figure A.1
Switching time for the capacitor circuit, if the capacitor value is the optimum one at $I_0 = 5$ A. With no precharging voltage, switching time is independent of the current, $\tau = \pi/2\omega$.

Resistor-Zener energy dissipation

The equation for the current is even simpler:

$$V_z + Ldi/dt + (R + R_1)i = 0,$$

whose solution is:

$$i = V_z/(R + R_1) + [I_0 - V_z/(R + R_1)] \exp(-t/\theta), \tag{4}$$

for the same initial conditions. θ is the time constant of the LR circuit: $L/(R + R_1)$. i will be zero for:

$$\tau = \theta Ln\{-[(R + R_1)I_0 - V_z]/V_z\}. \tag{5}$$

It must be remembered that V_z is negative for the fastest discharge.

The voltage across the coil will be maximum at $t = 0$, $U_{max} = V_z - R_1 I_0$, Fig. A.2 represents the variation of τ versus Zener voltage for $U_{max} = 1000$ V, resistor R_1 is given by $R_1 = (U_{max} - V_z)/I_0$. The optimum choice is $R_1 = 0$. The Zener diode and the resistor must be chosen to withstand the transient surge power imposed during the conduction, $P = V_z I_0$ for the diode, transient suppressors are well suited to this application, and $R_1 I_0^2$ for the resistor.

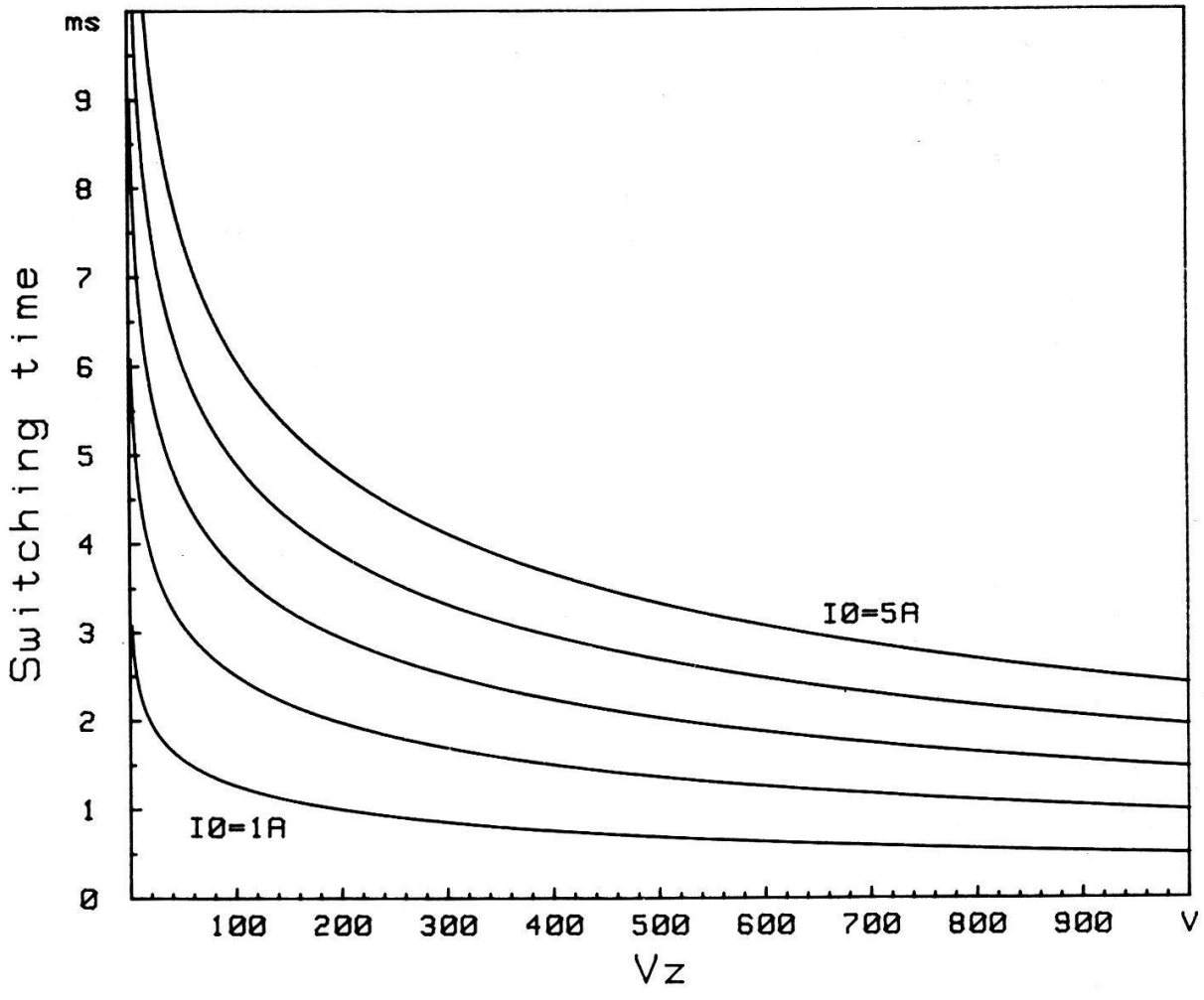

Figure A.2
Switching time for the Zener circuit, at $U_{max} = V_z + (R + R_1)I_0 = 1000$ V.

n of these circuits can be paralleled, the initial current into each cell will be I_0/n, and to allow an equal current repartition between the cells, a resistor R_1 must be used whose resistance will be higher than the Zener DC resistance. The switching time for this arrangement will be shorter, given by the curve for I_0/n. For instance, for the coil in this experiment, a 1000 V Zener will switch a 5A current in 2.4 ms. If it is replaced by 5×500 V Zener and $5 \times 500\ \Omega$ R_1 resistors, the energy will be removed in 0.7 ms. An additional advantage is the decrease of surge power requirements in the components by a factor n for the diodes and n^2 for the resistors.

In order to compare both methods, equations (3) and (5) can be reduced, with the assumption: $L^3C \ll 4R^2$ (capacitor circuit) and $R_1 = 0$ (Zener circuit), to:

$$\text{Capacitor: } \tau_1 = \frac{LI_0}{(U_{\max}^2 - U_0^2)^{1/2}} \operatorname{arctg} \frac{(U_{\max}^2 - U_0^2)^{1/2}}{U_0 + RI_0/2}.$$

$$\text{Zener: } \tau_2 = L/R \cdot Ln(1 + RI_0/U_{\max}).$$

The fastest rate for the capacitor circuit is achieved for U_0 close to $U_{\max}$ (Fig. A.1), and observing that for most coils $RI_0 \ll U_{\max}$. The usual approximations lead to:

$$\tau_1 \sim \tau_2 \sim LI_0/U_{\max}.$$

To emphasize these results, they can be applied to some existing coils, provided $U_{\max} = 1000$ V and exact calculations:

coil 1 (7) $L = 0.1$ H, $R = 1\ \Omega$ (at 77°K), $I_0 = 50$ A, $\tau = \tau_1 \sim \tau_2 = 4.89$ ms.
coil 2 (30) $L = 270\ \mu$H, $R = 0.1\ \Omega$ (room temperature), $I_0 = 500$ A, $\tau = 0.132$ ms.
coil 3 (this work) $L = 0.5$ H, $R = 15\ \Omega$ (room temperature), $I_0 = 5$ A, $\tau = 2.42$ ms.

It clearly appears that the best coil, from the switching rate point of view, will be that with the lowest LI_0 product for a given field.

REFERENCES

[1] R. KIMMICH, Bull. Magn. Res., *1,* 195 (1980).
[2] A. G. ANDERSON and A. G. REDFIELD, Phys. Rev., *116,* 3, 583 (1959).
[3] A. ABRAGAM, in "Principles of Nuclear Magnetism", Oxford Sc. Pub. (1983).
[4] G. J. BÉNÉ, B. BORCARD, E. HILTBRAND and P. MAGNIN, in "NMR Basic Principles and Progress", *19,* 81 (1981).
[5] R. KIMMICH and F. NOACK, Z. ANGEW, Phys., *29,* 4, 248 (1970).
[6] G. VOIGT and R. KIMMICH, Polymer, *21,* 1001 (1980).
[7] S. H. KOENIG and W. E. SHILLINGER, The J. of Biol. Chem., *244,* 12, 3283 (1969).
[8] D. P. WEITEKAMP, A. BIELECKI, D. ZAX, K. ZIHN and A. PINES, Phys. Rev. Let., *50,* 22, 1807 (1983).
[9] H. BENOIT and H. OTTAVI, Comp. Rend. Ac. Sc. B, 2708 (1960).
[10] Z. FLORKOWSKI, J. W. HENNEL and B. BLICHARSKA, Nukleonika, *14,* 6, 563 (1969).
[11] D. I. HOULT, in *Nuclear Magnetic Resonance Spectroscopy,* Emsley, Feeney, Sutcliffe, *12,* 41 (1979).
[12] J. E. ZIMMERMAN, J. App. Phys., *48,* 2, 702 (1977).
[13] J. G. GRAEME, in *Designing with Operational Amplifier,* MacGraw Hill (1977).
[14] B. F. MELTON and V. L. POLLACK, Rev. Sc. Inst., *42,* 6, 769 (1971).
[15] A. G. REDFIELD, W. FITE and H. E. BLEICH, Rev. Sc. Inst., *39,* 5, 710 (1968).
[16] W. WÖLFEL, Thesis, Stuttgart University, Minerva Publications Munich (1978).

[17] Transistor Data Book, National Semiconductor (1982).
[18] M. MERCK, R. SECHEHAYE, A. ERBÉIA and G. J. BÉNÉ, Mag. Res. Rel., 952 (1967).
[19] J. A. NELDER and R. MEAD, The Comp. J., *7,* 4, 308 (1965).
[20] MARQUARDT, J. Soc. Ind. Appl. Math., *11,* 2, 431 (1963).
[21] D. G. GARDNER, J. C. GARDNER, G. LAUSH and W. W. MEINKE, J. Chem. Phys., *31,* 4, 978 (1959).
[22] G. AUBARD, T. LENOIR, A. DENIS and P. CLAVERIE, Biophys. J. (in press).
[23] E. ROMMEL, G. OSSWALD, K. H. SCHWEIKERT and F. NOACK, 7th specialized Colloque Ampere, CIP Press Romania, 51 (1985).
[24] A. SZÖKE and S. MEIBOOM, Phys. Rev., *113,* 585 (1959).
[25] S. CONTI, Mol. Phys., *59,* 449 (1986).
[26] P. GILLIS and B. BORCARD, in press.
[27] A. ABRAGAM, *The Principles of Nuclear Magnetism,* 308–313 (1961).
[28] S. MEIBOOM, J. Chem. Phys., *34,* 2, 375 (1961).
[29] V. GRAF, F. NOACK and G. J. BÉNÉ, J. Chem. Phys., *72,* 2, 861 (1980).
[30] M. BLANZ, G. Q. CHEN, H. BIRLI and R. MESSER, 22nd Congress Ampere, 596 (1984).
[31] F. NOACK, Progress in NMR Spectroscopy, *18,* 171 (1986).
[32] D. K. LAI, thesis, Geneva (1986).
[33] B. BORCARD, in press.